JTTEE5 9:369-376

X-Ray Diffraction Characterization of Crystallinity and Phase Composition in Plasma-Sprayed Hydroxyapatite Coatings

Paul S. Prevéy

(Submitted 24 March 1997; in revised form 21 April 2000)

Orthopedic and dental implants consisting of a metallic substrate plasma spray coated with hydroxyapatite (HA) are currently used in reconstructive surgery. The crystalline phases present in the calcium phosphate ceramic and the degree of crystallinity must be controlled for medical applications. X-ray diffraction (XRD) is routinely employed to characterize the phase composition and percent crystallinity in both biological and sintered HA. However, application of the same XRD methods to plasma-sprayed coatings is complicated by the potential presence of several crystalline contaminant phases and an amorphous component.

To overcome the complexities of characterizing plasma-sprayed HA coatings, an external standard method of XRD quantitative analysis has been developed that can be applied nondestructively. Data collection and reduction strategies allowing separation of intensity diffracted from commonly occurring phases and the amorphous fraction are presented. The method is applied to coating samples, and detection limits and sources of error are discussed. Repeatability and accuracy are demonstrated with powder mixtures of known composition.

Keywords coatings, hydroxyapatite, quantitative phase analysis, x-ray diffraction

1. Introduction

Medical and dental implants employing hydroxyapatite (HA) plasma-sprayed coatings on a structural substrate are now widely used in reconstructive surgery. Both the crystallinity of the coating and the crystalline phase composition depend upon the plasma-spray processing parameters and are believed to affect the biological response to the ceramic coating.[1–4] To verify the phase composition achieved, x-ray diffraction (XRD) characterization of the coatings is recommended by the Food and Drug Administration[5] and required in ASTM F1185-88, "Standard Specification for Composition of Ceramic Hydroxylapatite for Surgical Implants."[6]

During the plasma-spray process, highly crystalline sintered HA powder is rapidly heated to a partially molten state and deposited at high velocity on a relatively cold metallic substrate, commonly the titanium alloy Ti-6Al-4V. Variation in either the plasma-spray conditions, particularly the thermal history, or in the composition of the starting HA powder can alter both the phase composition and crystallinity of the coating. The α or β forms of tricalcium phosphate (TCP), $Ca_3(PO_4)_2$, and calcium oxide (CaO) have been observed in plasma-sprayed coatings.[1–4,7]

X-ray diffraction methods have long been applied to characterize HA and related ceramic materials. However, the quantitative phase analysis methods described to date for plasma-sprayed HA coatings have usually been developed to measure specific features of the complex diffraction patterns, such as crystallinity or HA content, rather than providing complete phase analysis. The effects of variation in the mass absorption coefficients of the component phases are not addressed, or require an array of known mixtures for calibration. The crystallinity of biological or precipitated HA can be calculated from the XRD peak-to-background ratio of a mixture consisting of a single crystalline phase mixed with an amorphous fraction relative to that of a fully crystalline reference sample.[8,9] This method is not, however, generally applicable to plasma-sprayed coatings because of the potential presence of multiple phases.

The purpose of this paper is to describe an XRD quantitative phase analysis technique applicable to HA plasma-sprayed coatings based upon the reference intensity ratio (RIR) method commonly applied in mineralogy, which provides complete phase analysis,[10,11] modified to employ an external rather than an internal standard.

1.1 Prior Methods

Several methods have been described for determining the phase composition and the amorphous or glassy fraction generally present in HA plasma-sprayed coatings. In the method of LeGeros *et al.*,[12] the complex diffraction patterns produced by plasma-sprayed coatings are deconvoluted for phase quantification, but the broad diffraction peak tails are truncated, leaving uncertainties in the integrated intensity. Relative intensities reported in the JCPDS files are used in quantification rather than true reference intensity ratios, and the effect of the absorption coefficients of the component phases upon the intensity of the diffraction peaks is not considered. A similar method is described by Burgess *et al.*,[13] but calibration with known mixtures is used to account for absorption effects. Calibration curves are suitable for mixtures of two components but are impractical for generalized mixtures of several component phases, which commonly occur in plasma-sprayed HA coatings.

Paul S. Prevéy, Lambda Research, Cincinnati, OH 45227. Contact e-mail address: pprevey@lambda-research.com.

Keller and Rey-Fessler[14] have described a parallel beam XRD method developed for cylindrical samples. This procedure determines the percent crystallinity from calibration curves developed from mixtures of fully crystalline and "fully amorphous" powders. Because the HA coating need not be removed from the metallic substrate, the method of Keller and Rey-Fessler provides nondestructive determination of the phase composition. Flach, *et al*.[15] describe a similar method in which coatings are characterized using calibration curves derived from known mixtures of 100% crystalline and "100% amorphous" material. Keller and Dollase[24] propose a method similar to Keller and Rey-Fessler[14] and note a strong dependence of the calibration constant derived from the mixtures of amorphous and crystalline material upon the range of integration used in measuring the integrated intensities. These methods rely upon calibration curves requiring fully amorphous material produced by splat cooling of molten powders. The lowest energy state of a solid phase is the fully crystallized state, which is well defined by diffraction peak widths reduced to the limits of instrumental broadening. Fully crystalline HA powder is easily achieved by annealing. In contrast, the nature of the amorphous glassy phase developed by rapid cooling during plasma-spray deposition is inconsistent (dependent upon temperatures and cooling rates) and may not be stable. Calibration using an amorphous standard is, therefore, specific to the plasma-spraying conditions used to produce the amorphous or glassy standard and is not generally applicable. By quantifying all of the crystalline phases and calculating the amorphous fraction as the balance remaining, as proposed here, the uniformity and nature of the amorphous fraction need not be considered.

The Rietveld method,[25] in which a model of the crystal structure is refined by least-squares techniques to fit the full diffraction pattern, has found broad applications in powder diffraction. Keller[17] has applied Rietveld analysis to the complex mixture of amorphous and crystalline phases in HA plasma-sprayed coatings. When used for quantitative analysis of HA coatings, the method is shown to produce solutions that are not unique, but depend upon the initial estimates of the large number of parameters assumed in the analysis. To achieve a satisfactory fit, it is necessary to adopt an arbitrary complex background function (that does not coincide with the scattering maximum of the amorphous fraction) and temperature factors, B_j, that differ markedly for the starting powder and deposited coatings. No physical basis appears to exist for either of these features of the solution. The method fails to quantify the poorly crystalline β-TCP that is the common secondary phase found in plasma-sprayed coatings.

1.2 The Nature of the Poorly Crystallized or Amorphous Fraction

Poorly crystallized or truly amorphous material commonly comprises from 10 to 50 vol.% of typical plasma-sprayed HA coatings. The available phase quantification methods treat this significant fraction of the coating differently. Some include it in the calculation of the crystalline fraction, while others exclude it as a separate noncrystalline phase. The broad diffraction peaks seen in the diffraction patterns of plasma-sprayed coatings may be treated as "microcrystalline" HA, with crystallite sizes on the order of 10 Å, and included in the calculation of the crystalline fraction.[12] Alternately, the fraction has been treated as a separate Ca/P glassy phase formed by the rapid splat cooling of the semimolten HA powder and excluded from the crystalline fraction.[14,16] Clearly, the true nature of this fraction must first be established before phase quantification.

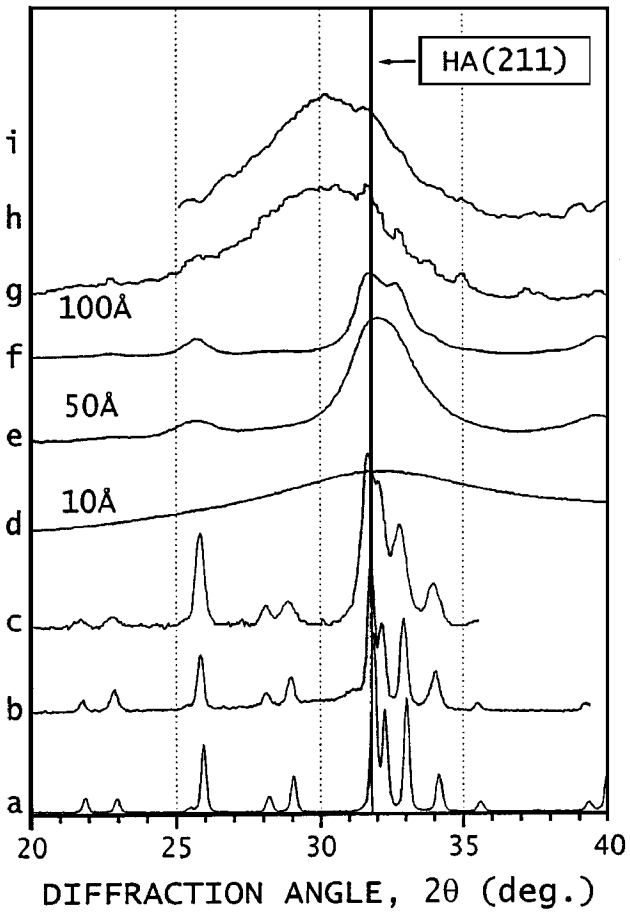

Fig. 1 Diffraction patterns taken from a variety of sources as noted, digitized, and replotted on a common angular scale to differentiate the a morphous Ca/P glassy phase from the broadened peaks of microcrystalline HA. (**a**) Fully crystalline sintered HA. (**b**) Hydroxyapatite plasma-spray coating containing crystalline and glassy material. (**c**) Hydroxyapatite prepared as a precipitate with a small crystallite size (material provided by Dr. L. Kuhn Spearing). (**d**) to (**f**). Calculated diffraction patterns produced by crystalline HA with 10, 50, and 100 Å after Keller.[22] (**g**) Highly amorphous coating produced on a dental implant containing a minor crystalline fraction (materials provided by Dr. Paul Glick). (**h**). Highly amorphous calcium phosphate glass from Flach, *et al*.[15]

Naturally occurring HA obtained from bone or poorly crystallized HA produced by precipitation[23] shows very broad diffraction peaks produced by crystallite sizes estimated in the range of tens to hundreds of Angstroms. Diffraction patterns of highly crystalline sintered HA, and the small crystallite sizes developed during precipitation, are shown in Fig. 1(a) and (c). A typical diffraction pattern for a plasma-sprayed HA coating is shown in Fig. 1(b).

Work by Keller[22] using Rietveld techniques to simulate the diffraction patterns of HA has shown that reduction in crystallite sizes to dimensions on the order of 10 Å causes broadening, very similar to natural or precipitated HA, but no shift in the an-

gular positions of the broadened diffraction peaks. Figure 1(d) to (f) shows Keller's calculated diffraction peaks for a range of crystallite sizes from 10 to 100 Å, presented on the same angular scale.

The diffraction patterns reported by several authors for plasma-sprayed coatings containing a large fraction of poorly crystallized material are presented normalized and on a uniform angular scale in Fig. 1(g) and (h). Comparison of Fig. 1 (g) and (h) with the calculated patterns of Fig. 1(d) to (f), and the microcrystalline HA of Fig. 1(c), clearly reveals that the broad maximum found in plasma-sprayed coatings is shifted nearly 2°, to lower Bragg angles, than the (211) diffraction peak produced by crystalline HA, regardless of the crystallite size. The structure of the amorphous fraction of plasma-sprayed coatings is distinctly different from that of microcrystalline HA and is attributed to a separate glassy Ca/P phase produced by rapid cooling during plasma spraying. Keller and Dollase [24] report the amorphous maxima at 30.5°. Using a combination of XRD and optical microscopy to examine HA plasma-sprayed coatings produced under a wide range of conditions, Gross and Brendt[18] have also concluded that a noncrystalline glassy phase is produced during the thermal cycle and rapid cooling of the plasma-spray process.

This paper describes a method of XRD quantitative phase analysis using an external standard RIR method. The method has been derived from the fundamental physical principles of XRD and allows simultaneous determination of the weight or volume fractions of HA (including microcrystalline material), both the α and β forms of (TCP), and CaO. The Ca/P glassy phase is treated as a separate component of the multiphase system comprising the balance of the material in the coating. "Microcrystalline" HA is included in the contribution to the long tails of the broadened HA diffraction peaks. The percent crystallinity is calculated as the sum of the weight fractions of the crystalline phase fractions, excluding the glassy Ca/P fraction.

2. Selection of the External Standard Method

The intensity of XRD from any system of phases is given as a function of the diffracting volume of each phase by the powder pattern power theorem.[19] If the effects of variation in the absorption coefficient of the mixture on the diffracted intensities are included, the volume fraction of any crystalline phase in a mixture can be calculated from the measured integrated intensities of diffraction peaks produced by the component phases. The need for empirical calibration is then eliminated, and mixtures containing several phases in any proportion can be analyzed.

X-ray diffraction quantitative phase analysis can be performed by one of three fundamental methods: direct comparison, internal standard, and external standard.[10,20] The direct comparison method requires no reference standard but is only applicable to fully crystalline samples, or with prior knowledge of the sample crystallinity. Plasma-sprayed HA coatings generally contain a significant glassy Ca/P fraction, prohibiting use of the direct comparison method. Both the internal and external standard methods are applicable to samples containing an unknown amorphous fraction. Because the internal standard method requires no prior knowledge of the sample composition, it is generally preferred for XRD quantification.[11] However, it is only applicable to finely powdered samples into which a measured amount of a crystalline standard can be uniformly mixed. The external standard method can be applied without disturbing the sample, but only if the mass absorption coefficient of the mixture of phases is known.

The external standard method has been selected because it is applicable to partially amorphous multiphase solid samples of known chemical composition, such as plasma-sprayed coatings. The elemental composition of the plasma-sprayed coating is the same as the starting powder. Therefore, the mass absorption coefficient of the HA plasma-sprayed coating to be analyzed is equal to the known coefficient of the starting HA powder. The diffraction pattern obtained nondestructively from the coating surface is quantified with reference to an external standard such as aluminum oxide or quartz powder. The percent crystallinity of the multiphase coatings is taken to be the sum of all crystalline fractions present. The balance remaining is the amorphous fraction.

2.1 The External Standard Method

If the diffracted intensity from a pure sample of a phase i is I_i, and the intensity I_i is measured under identical experimental conditions from a mixture containing an unknown weight fraction W_i of phase i, then the weight fraction in the unknown mixture can be calculated from the ratio of the integrated intensities as

$$W_i = \frac{I_i}{I_i^p} \cdot \frac{(\mu/\rho)_m}{(\mu/\rho)_i} \qquad \text{(Eq 1)}$$

where $(\mu/\rho)_i$ and $(\mu/\rho)_m$ are the mass absorption coefficients for the pure phase and the mixture, respectively. Equation 1 is the working equation for the external standard method. The mass absorption coefficient of the mixture, $(\mu/\rho)_m$, must be known independently. In the special case of application to plasma-sprayed coatings, because the elemental compositions of the coating and the starting powder remain the same, regardless of any phase transformations, the mass absorption coefficient of the coating will be equal to that of the starting powder.

2.2 The External Standard Method Using Reference Intensity Ratios

The complexity of the analysis of multiple phases in a mixture can be greatly reduced if all of the pure phase peak intensities are referenced to a single standard. The RIR for a phase i is defined as:

$$\mathrm{RIR}_i = \frac{I_i}{I_s}$$

where I_i is the intensity of the 100% peak of phase i, and I_s is the intensity of the 100% peak of a reference phase s, taken by convention to be α-Al_2O_3, corundum, in a 50:50 mixture by weight.

For an external standard, the RIR values must be expressed in terms of the pure intensities, rather than the intensities in a mixture. From Eq 1, the ratio of the intensities of the strongest lines of phases i and s in a mixture is:

$$\frac{I_i}{I_S} = \frac{W_i}{W_s}\frac{I_i^p}{I_s^p}\frac{(\mu/\rho)_i}{(\mu/\rho)_s}$$

In a 50:50 mixture by weight, $W_i = W_s$, the ratio of intensities is, by definition, the RIR value:

$$\frac{I_i}{I_{s50:50}} = \frac{I_i^p}{I_s^p}\frac{(\mu/\rho)_i}{(\mu/\rho)_s} \equiv \mathrm{RIR}_i \qquad \text{(Eq 2)}$$

Solving Eq 2 for I_i^p in terms of its RIR value and substituting into Eq 1 yields the weight fraction of phase *i* in terms of the ratio of the strongest (100%) peaks of the *i*th and reference phases.

$$W_i = \frac{I_i}{I_s^P}\frac{(\mu/\rho)_m}{(\mu/\rho)_s}\frac{1}{\mathrm{RIR}_i} \qquad \text{(Eq 3)}$$

The integrated intensity of any diffraction peak from a phase with arbitrary Miller indices (*hkl*) can be expressed as a fraction of the intensity of the strongest diffraction peak, I_i, of that phase by the relative intensity. Equation (3) can then be generalized as:

$$W_i = \left[\frac{I_i^{hkl}}{I_i^{REL}}\right]\cdot\left[\frac{(\mu/\rho)_m}{(\mu/\rho)_s}\right]\cdot\left[\frac{1}{I_s^p \cdot \mathrm{RIR}_i}\right] \qquad \text{(Eq 4)}$$

where I_i^{hkl} is the measured integrated intensity of the (*hkl*) reflection for phase *i*, and I_I^{REL} is the relative intensity of (*hkl*) reflection for phase *i*.

If the RIR values for all components in a mixture are known relative to the reference phase, *s*, a single determination of I_s^p in conjunction with the measurement of I_i^{hkl} under identical experimental conditions allows solution of the entire system of weight fractions, W_i. The use of RIR values is much faster and less prone to error than the determination of all of the weight fractions from Eq 1, which would require reference to the integrated intensities of the 100% peak of each phase in its pure form.

For samples containing an amorphous fraction, the percent crystallinity is determined as the sum of all the weight fractions of the crystalline phases in the mixture, which will be less than unity.

3. Experimental Method

X-ray diffraction data were acquired using copper K_a radiation, a graphite diffracted beam monochromator, and a scintillation detector on a Bragg-Brentano focusing diffractometer. The x-ray source was a conventional sealed 2500 W x-ray tube operated at 50 kV and 40 mA. Incident and diffracted beam slits were 1.0 and 0.2°, respectively, chosen for high intensity. Data were collected by step counting at 0.02° intervals for 2 seconds per data point.

3.1 Experimental Determination of RIR Values

The RIR values were determined using commercially available pure samples of HA, β-TCP, and CaO. Pure α-TCP could not be obtained, and only a mixture containing a small fraction of β-TCP was available. The RIR value for α-TCP was obtained from the mixture of α- and β-TCP after quantification of the amount of β-TCP in the mixture. Alpha-quartz, rather than α-Al_2O_3, was selected initially as a suitable internal standard because peak interference was minimal, and finely ground (5 μm) pure powder was readily available as a stable reference standard. Mixtures were prepared for measurement of the intensity ratios needed for the calculation of RIR values for each phase. At least five runs were made for each phase, with the powder samples remixed and repacked in the sample holders between each run to reduce errors due to inhomogeneity of the powder mixtures. The mean and standard deviations for RIR values calculated for each phase are presented in Table 1.

Table 1 (RIR) relative to alpha quartz and corundum

	RIR value	
Phase	**α-Quartz**	**Corundum**
Hydroxyapatite (a)	0.315(3)	
(b)	0.296(2)	1.276(8)
α-TCP	0.20(1)	0.87(4)
β-TCP	0.266(9)	1.15(4)
CaO	0.783(6)	3.37(2)

(a) Commercial sintered HA powder
(b) Laboratory precipitate preparation

The RIR values of a commercial sintered HA plasma-spray starting powder and a laboratory precipitate preparation were found to differ by approximately 6%. Both samples were free of any contaminants detectable by XRD and were obtained as "pure" HA powders. Minor variation or substitution in the apatite structure is assumed to alter the structure factor and the RIR values measured for the two samples. It is generally recommended that RIR values be determined experimentally for any phase using the data reduction methods and instruments to be employed for measurement.[21]

3.2 Data Reduction Strategy

Known mixtures of HA, α-TCP, β-TCP, and CaO were prepared to develop a data collection and reduction strategy in which the angular regions of peak integration and background were selected. The known mixtures were also used to test the validity of the RIR values and relative intensities. A typical diffraction pattern for a mixture containing 85% HA and additional contaminant phases, as indicated, is shown in Fig. 2.

Plasma-sprayed HA coatings can vary widely in the amount of the glassy Ca/P phase producing the broad amorphous peak near 30°. The broad, diffuse peak from the glassy phase was approximated by fitting a Pearson VII function profile over a range sufficient to define the contribution of the broad tails. Much narrower Pearson VII functions were used to define the contribution of the neighboring HA peaks to the combined diffraction pattern. Peak profile fitting of the height, position, width, and the power term independently for each peak was performed using the method of Gupta and Cullity[26] assuming a K_α doublet. The deconvolution of the overlapping peaks is shown in Fig. 3. After examination of the diffraction patterns of both the known mixtures and actual coating samples, regions of true background, beyond the tails of the broad glassy Ca/P peak, were selected, which would be suitable for analysis of any likely concentrations of the phases encountered in plasma-sprayed HA coatings. The following data reduction strategy was developed for acquiring the integrated intensities necessary to quantify mixtures of α-TCP, β-TCP, CaO, and HA. (Provision is made for interference

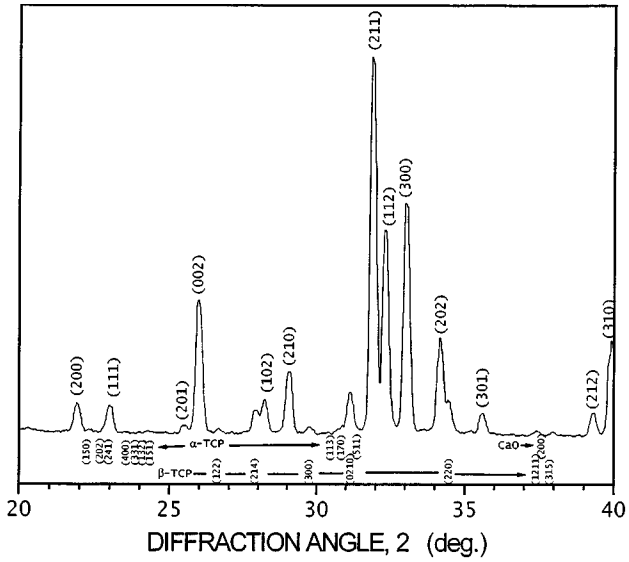

Fig. 2 Diffraction pattern of the nominally 85% HA fully crystalline known mixture with the principal diffraction peaks of the phases i dentified. Actual composition is shown in Table 3

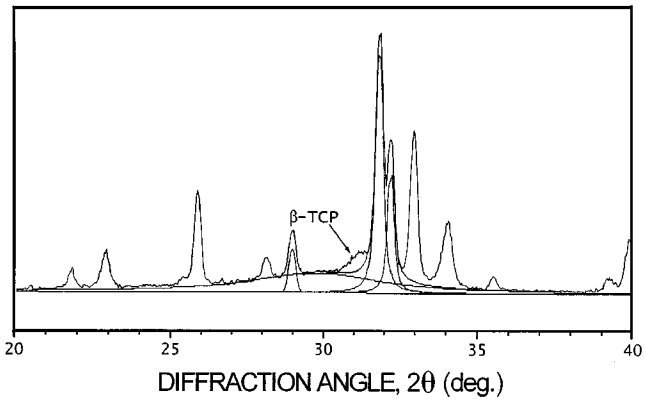

Fig. 3 Deconvolution of diffraction peaks and the amorphous glassy Ca/P phase using Pearson function peak approximation on a linear background to recover the β-TCP contribution. The β-TCP integrated intensity is obtained as the balance remaining after subtraction of the contributions from the glassy phase in the well-crystallized HA material

Table 2 Combined relative intensities for the integration regions indicated

Crystalline phase	2 θ range	I^{REL}
Hydroxylapatite	38.5–59.0.	2.16(2)
α-TCP	23.8–24.8	0.462(3)
	29.3–30.2	0.211(2)
	30.5–31.6	1.26(2)
	38.5–59.0	2.15(1)
β-TCP	30.5–31.6	1.00
	37.0–38.5	0.145(1)
	38.5–59.0	2.35(1)
CaO	37.0–38.5	1.00
	38.5–59.0	1.32(1)

effects from β-$Ca_2P_2O_7$, but this phase has not been observed in plasma-sprayed coatings in this laboratory, and RIR values have yet to be determined.)

- The α-TCP content is obtained by integrating the α-TCP (331), (132), and (151) peaks from 23.8 to 24.8°. This region is free from interference from any other phase likely to be found in HA samples. A quadratic background is assumed.
- The (008), (210), and (211) β-$Ca_2P_2O_7$ peaks are integrated from 29.3 to 30.20° to allow calculation of the intensity of the 100% peak. No pure sample of this phase has been available to allow the development of RIR values for quantification, but the integrated intensities may be corrected for interference. The integrated intensity will be in error due to interference from the β-TCP (300) and the α-TCP (113) peaks. This region is integrated assuming a linear background and a Pearson VII functional form of the peaks surrounding the region, including the diffuse peak attributed to the glassy Ca/P material.
- The β-TCP content is obtained by integration from 30.5 to 31.5°. The region is corrected for α-TCP (170) and (511) peak interference and possible β-$Ca_2P_2O_7$ (204) and (212) interference, if present. The β-TCP peak being used for quantification is the (0210) peak. This region is integrated in the same fashion as the β-$Ca_2P_2O_7$ peaks above.
- The calcium oxide content is determined by integration from 37.0 to 38.5° with correction for the β-TCP (1211) and (315) peaks. This region contains the 100% (200) calcium oxide peak and is integrated assuming a quadratic form to the background.
- Finally, the entire region from 38.5 to 59° is integrated assuming a linear background and corrected for interference by α-TCP, β-TCP, calcium oxide, and possibly β-$Ca_2P_2O_7$ to obtain the HA content. Many peaks are included in the integration range to reduce the effects of preferred orientation.

3.3 Relative Intensities

The relative intensities of the peaks or peak regions used in the analysis were obtained by direct measurement of samples of each phase. The integrated intensities were calculated from Pearson VII function peak profiles fitted by regression after background subtraction. Table 2 summarizes the combined fractional relative intensities for each phase summing all of the peaks found within the integration ranges shown. The HA values are the averages of results from pure samples obtained from five different sources.

4. Analysis of Calcium Phosphates

4.1 Known Mixture Tests

The data collection strategy and the integrity of the experimentally determined values of RIR and I_{REL} were tested by quantifying the known mixtures. Because no amorphous fraction was present in the known mixtures, the external standard method was reduced to a direct comparison method (100% crystallinity is assumed).

One mixture containing nominally 85% HA, 10% β-TCP, 3% α-TCP, and 2% CaO was prepared to closely simulate the nom-

Table 3 Repeatability test on a known mixture

Trial	% HA	% β-TCP	% α-TCP	% ($\alpha+\beta$)TCP	%CaO
Sample 1					
1	87.1	8.5	4.2	12.7	0.2
2	86.2	10.5	3.1	13.6	0.2
3	86.6	13.0	0.4	13.4	0.05
4	87.8	12.0	0.2	12.2	0.08
5	87.1	6.4	6.1	12.5	0.3
6	86.1	12.6	1.3	13.9	0.08
Average	86.8 ± 0.6	10.5 ± 2.6	2.5 ± 2.3	13.0 ± 0.6	0.2 ± 0.1
Actual	84.9	10.1	3.0	13.1	2.0
Sample 2					
1	67.6 ± 1.6	15.9 ± 0.9	12.8 ± 0.7	28.7 ± 1.5	3.4 ± 0.1
Actual	69.7	15.1	10.0	25.1	5.2

inal composition of actual plasma-spray coatings containing small amounts of contaminants in a relatively pure HA matrix. Six repeat trials were made, remixing and repacking the powder sample between each measurement to include any effects of microabsorption, inhomogeneity, and texture produced by packing the powder. The results, presented in Table 3, demonstrate both the accuracy and the repeatability of the method using the data reduction strategy on well-crystallized samples. Repeatability within 1 wt.% was observed for the major HA phase and within 3 wt.% for the minor α-TCP and β-TCP phases. The average weight fraction obtained was within 3 wt.% of the actual measured values for each phase.

The high relative error in the determination of the individual α-TCP and β-TCP fractions is due to uncertainty in separation of the contributions of each phase to the 30.5 to 31.6° integration range when only small quantities of the α-TCP phase are present. If only the combined fraction of the two phases is reported, the error is greatly reduced. The combined fractions of α-TCP and β-TCP phases are 13.0 ± 0.6 wt.%. The actual combined fraction is 13.1%.

The second known mixture containing nominally 70% HA and larger fractions of the other phases was measured only once, as shown at the bottom of Table 3. Based upon comparison to the known weight fractions and the error propagated for the calculation of the fraction of the individual phases, the accuracy is comparable to that achieved for the 85% sample.

The consistently low results obtained for CaO are not fully understood. The reagent grade material used as a standard was observed to be hygroscopic. Compressed pure pellets absorbed water rapidly and nearly doubled in size over a period of a few days. The thin layer of powder penetrated by the x-ray beam at the sample surface may have been similarly affected after preparation of the known mixtures, reducing the intensity of the CaO diffraction peaks and the weight fraction calculated.

4.2 Plasma-Sprayed Coatings

The external standard method was used to analyze nine HA plasma-sprayed coating samples reportedly obtained from a variety of commercial sources and representing a wide range of both dental and prosthetic applications, as well as experimental coatings. The set of coating samples was provided by a client for XRD characterization and demonstration of the proposed method of quantitative phase analysis. The origin of the individual samples was not provided to ensure a blind evaluation. The results are reported here to show application of the method to a variety of commercial coatings and to demonstrate performance on a wide range of compositions.

Table 4 Quantitative phase analysis of nine plasma-sprayed coatings

Sample	% HA	% β-TCP	% α-TCP	% CaO	% Crystallinity
1	48 ± 5	5 ± 2	2 ± 0.8	0.0 ± 0.2	54.9
2	66 ± 5	2 ± 1	1 ± 0.6	0.0 ± 0.2	68.8
3	80 ± 6	2 ± 2	2 ± 0.7	0.1 ± 0.2	83.6
4	50 ± 5	6 ± 2	0.1 ± 0.8	0.0 ± 0.3	55.3
5	32 ± 5	5 ± 2	0.1 ± 0.8	0.4 ± 0.2	37.3
6	60 ± 3	4 ± 1	0.0 ± 0.8	0.0 ± 0.1	64.6
7	48 ± 5	5 ± 2	1.0 ± 0.7	0.0 ± 0.2	53.4
8	62 ± 3	5 ± 1	0.0 ± 0.8	0.0 ± 0.1	66.8
9	33 ± 2	5 ± 1	0.0 ± 0.7	0.3 ± 0.1	37.7

All the HA coating samples were analyzed nondestructively, mounting the coated substrates in a flat sample holder. A 1° incident beam was used in a constant incident angle mode, allowing the width of the irradiated area to decrease with increasing diffraction angle. Using Cu K_α radiation and a graphite monochromator, as detailed above, the irradiated area ranged from nominally 10 × 12 mm at the lowest diffraction angle of 20° to 10 × 5 mm at the highest angle of 60°. A quartz external standard was measured concurrently using the same experimental conditions.

The results for the plasma-sprayed coating samples are presented in Table 4 and graphically in Fig. 4. The crystallinity, taken as the sum of the crystalline fractions of the samples, varied from 38% to 84%. The most common secondary phase was β-TCP, which was observed in all of the coating samples, ranging from nominally 2% to 6%. Up to 2%, α-TCP was attributed to four of the samples, but as noted above, the combination of the two TCP components is more reliable. No significant amount of CaO was observed in any of the coatings.

The error calculated for the determination of the major HA fraction in the coatings is higher (ranging from 2% to 6% for the individual samples) than that reported for the known mixtures (0.6% and 1.6%) in Table 3. Diffraction from the glassy Ca/P phase, which exceeded 60% of the material in some of the coatings, must be subtracted from the contribution of the other phases introducing error in the determination of the net integrated intensities of all of the phases. The glassy phase does not occur in the fully crystalline known mixtures. The fraction of HA is calculated by subtracting the contributions from all of the other phases from the extended integration range, compounding the error in measurement.

A deficiency of the data reduction scheme currently employed is the sensitivity to the contribution of the secondary maximum of the amorphous glassy material to the long integration range (38.5 to 59°) used to quantify the HA component. Integration of the full diffraction pattern obtained from the amorphous material produced by plasma-spray deposition (Fig. 1g) reveals that the secondary maximum is on the order of 12% of the intensity of the primary, using the integration ranges proposed. For a typical HA plasma-sprayed coating with a crystalline HA content on the order of 70%, the error due to the secondary maximum would be on the order of 4% of the HA content reported, less than the nominal random error for mea-

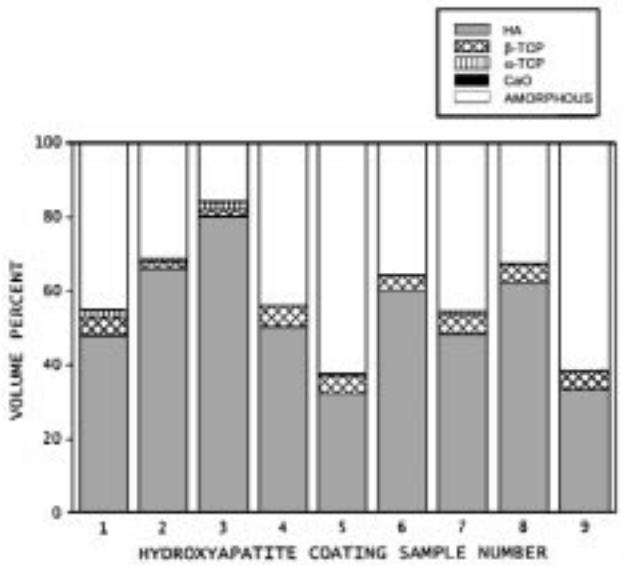

Fig. 4. Bar chart showing the range of amorphous glassy calcium phosphate phase and contaminate phases in nine plasma-spray coating specimens representing a range of commercial and experimental coatings

surement of coatings. Because the intensity of the primary maximum is measured in the analysis, the method could be improved and applicability extended to coatings of lower crystallinity by correcting for the interference from the secondary amorphous maximum.

5. Conclusions

A nondestructive method for quantitative phase analysis by XRD has been developed to determine the amount of HA, α-TCP, β-TCP, CaO, and the amorphous CA/P glassy phase in plasma-sprayed HA coatings. The crystallinity of the sample is calculated as the sum of the crystalline fractions present in the coating, with the balance being amorphous. A layer of nominally 25 μm is sampled allowing direct analysis of the surface of dental and orthopedic coatings, which will be placed in contact with tissue. The method uses the integrated intensity of several diffraction peaks of each phase to minimize the effects of preferred orientation.

The method has been shown to provide both reproducibility and accuracy on the order of ± 2% for the HA, CaO, and TCP in known fully crystalline mixtures. Individual accuracies for the α- and β-TCP fractions are relatively lower because of the method of phase separation. Uncertainties increase to ±5% for the HA content of plasma-sprayed coatings containing up to 50% amorphous material.

Acknowledgments

The author gratefully acknowledges the assistance of Mr. Rick Georgette, Bio-Coat, Inc., for assistance in obtaining the pure powder samples and of Drs. Liisa Kuhn Spearing and Dr. Paul Glick for providing the HA materials. Data, correspondence, and many helpful discussions with the members of ASTM Committee F04.13.05, especially Mr. Floyd Larson and Drs. Paul Glick, Dr. Liisa Kuhn Spearing, and Dr. Ludwig Keller, contributed to the development of the method and are much appreciated.

References

1. R.G. LeGeros: *Calcium Phosphates in Oral Biology and Medicine,* S. Karger AG, Basel, Switzerland, 1991, Chapter 4, pp. 68-81.
2. S. Radin and P. Ducheyne: in *Characterization and Performance of Calcium Phosphate Coatings for Implants,* ASTM STP 1196, Emanuel Horowitz and Jack E. Parr, eds., ASTM, Philadelphia, PA, 1994, pp. 111-23.
3. K.A. Gross and C.C. Berndt: in *Characterization and Performance of Calcium Phosphate Coatings for Implants,* ASTM STP 1196, Emanuel Horowitz and Jack E. Parr, eds., ASTM, Philadelphia, PA, 1994, pp. 124-39.
4. P. Ducheyne and S. Radin: in *Characterization and Performance of Calcium Phosphate Coatings for Implants,* ASTM STP 1196, Emanuel Horowitz and Jack E. Parr, eds., ASTM, Philadelphia, PA, 1994, pp. 140-48.
5. T.J. Callahan, J.B. Gantenberg, and B.E. Sands: in *Characterization and Performance of Calcium Phosphate Coatings for Implants,* ASTM STP 1196, Emanuel Horowitz and Jack E. Parr, eds., ASTM, Philadelphia, PA, 1994, pp. 185-97.
6. *Annual Book of ASTM Standards,* ASTM, Philadelphia, PA, 1988, vol. 13.01.
7. R.Z. LeGeros, R. Zheng, R. Kijkowska, D. Fan, and J.P. LeGeros*: in Characterizations and Performance of Calcium Phosphate Coatings for Implants,* ASTM STP 1196, Emanuel Horowitz and Jack E. Parr, eds., ASTM, Philadelphia, PA, 1994, pp. 43-53.
8. R.G. LeGeros: in *Calcium Phosphates in Oral Biology and Medicine,* S. Karger AG, Basel, Switzerland, 1991, p. 27.
9. A. Posner and F. Betts: *Acc. Chem. Res.,* 1975, vol. 8, pp. 273-81.
10. H.P. Klug and L.E. Alexander: *X-ray Diffraction Procedures,* 2nd ed., John Wiley & Sons, New York, NY, 1974, pp. 541-54.
11. R. Snyder and D. Bish: in *Modern Powder Diffraction, Reviews in Mineralogy,* D.L. Bish and J.E. Post, eds., The Mineralogical Society of American, Washington, DC, 1989, vol. 20, pp. 101-22.
12. J. LeGeros, R. LeGeros, A. Burgess, B. Edwards, and J. Zitelli: in *Characterization and Performance of Calcium Phosphate Coatings for Implants,* ASTM STP 1196, Emanuel Horowitz and Jack E. Parr, eds., ASTM, Philadelphia, PA, 1994, pp. 33-42.
13. A. Burgess, D. La, and W. Wagner: "A Refinement and Evaluation of a Method for the Quantitative Characterization of Calcium Phosphate Coatings," presented to ASTM Committee F04.13.05 for consideration, May 1993.
14. L. Keller and P. Rey-Fessler: in *Characterization and Performance of Calcium Phosphate Coatings for Implants,* ASTM STP 1196, Emanuel Horowitz and Jack E. Parr, eds., ASTM, Philadelphia, PA, 1994, pp. 54-62.
15. J.S. Flach, L.A. Shimp, C.A. van Blitterswijk, and K. de Groot: in *Characterization and Performance of Calcium Phosphate Coatings for Implants,* ASTM STP 1196, Emanuel Horowitz and Jack E. Parr, eds., ASTM, Philadelphia, PA, 1994, pp. 25-32.
16. P.S. Prevey and R.J. Rothwell: in *Characterization and Performance of Calcium Phosphate Coatings for Implants,* ASTM STP 1196, Emanuel Horowitz and Jack E. Parr, eds., ASTM, Philadelphia, PA, 1994, pp. 63-79.
17. L. Keller: *J. Biomed. Mater. Res.,* 1995, vol. 29, pp. 1403-13.
18. K.A. Gross and C.C. Berndt: *Bioceramics 8,* Butterworth-Heinemann, London, 1995, pp. 361-366.
19. B.E. Warren: *X-ray Diffraction,* Addison-Wesley, Reading, PA, 1968, p. 49.
20. F.H. Chung: *Adv. X-ray Analysis,* 1973, vol. 17, pp. 106-15.
21. *Modern Powder Diffraction,* Review in Mineralogy 20, D.L. Bish and

J.E. Post, eds., Mineralogical Society of America, Washington, DC, 1989, pp. 106 and 109.
22. L. Keller and S. Iyengar: "XRD Phase Analysis of Ca-Phosphate Coatings Using the Rietveld Method," presented to ASTM Committee F04.13.05, Dallas, TX, November 1993.
23. R.Z. LeGeros: in *Calcium Phosphates in Oral Biology in Medicine*, S. Karger AG, Basel, Switzerland, 1991, pp. 8, and 9.
24. L. Keller and W.A. Dollase: *J. Biomed. Mater. Res.*, 2000, vol. 49, p. 244.
25. *The Rietveld Method*, IUC Monographs on Crystallography 5, R.A. Young, ed., International Union of Crystallography, Oxford University Press, Oxford, United Kingdom, 1993.
26. S.K. Gupta and B.D. Cullity: *Adv. X-ray Analysis*, 1980, vol. 23, p. 333.